Packaging of a High-Speed Optical Modulator using Flip Chip Interconnects

Y. S. Visagathilagar[*1], W. S. T. Rowe[*1], A. Mitchell[*1], G. Bennett[*2] and M. Grosser[*2]
[*1]Australian Photonics CRC,
School of Electrical and Computer Engineering, RMIT University,
GPO Box 2476V, Melbourne, Victoria 3001, Australia.
Phone (+613) 9925 2896; Fax (+613) 9662 1921
Email: yuvaraja@rmit.edu.au

[*2]Defence Science and Technology Organisation (DSTO),
P. O. Box 1500, Edinburgh, South Australia 5111, Australia.

Abstract

Optical modulators using "Lithium Niobate" ($LiNbO_3$) have become the industry standard for high-speed data transmission and RF photonic links. Packaging is a determining factor in maintaining low cost and high-performance. This paper investigates the application of flip chip technology to optical modulator packaging. Experimental results show that rugged flip chip bonds can be realized with minimal impact on the modulator electrical performance.

I. Introduction

Current telecommunication and defense applications utilize high-speed optical modulators for the distribution of RF/microwave signals over optical fiber. Advantages include large electrical bandwidth, immunity to interference and robust system construction [1]. High-speed optical modulators can be implemented on $LiNbO_3$ using a Mach-Zehnder Interferometer (MZI) configuration [2,3]. A limiting factor on the bandwidth of a high-speed MZI is the RF/optical packaging [4]. Packaging is also a significant factor in determining the cost to manufacture these devices.

$LiNbO_3$ is an unusual material that is brittle and is very temperature sensitive [5]. Packaging of devices to accommodate these materials properties can be challenging. Typical MZI chips also have awkward dimensions (i.e. 60 x 2 x 0.25mm) in order to maximise efficiency and eliminate substrate resonances [6]. The high aspect-ratio and fragility of these chips further complicate the task of packaging.

Traditionally, high-speed modulators are electrically interfaced using wire or ribbon bonding techniques to connect the modulator electrodes to the external RF connectors [4]. This technique is labor intensive, and can consume a significant proportion of the total package volume. The geometry of the MZI electrodes also imposes constraints on the package design. Figure 1 presents diagrams of several proposed modulator electrodes including a single electrode and dual electrode [3], and arrays of MZI's [7]. The electrode is bent to enable edge access for wire bonding, as shown in Figure 1(a). This results in an inefficient use of valuable substrate real-estate and can degrade performance due to excess conductor loss on the high dielectric constant $LiNbO_3$ substrate. This problem becomes particularly acute when attempting to implement dense modulator arrays [7] as shown in Figure 1(c).

An investigation into a suitable package for these modulators is required to satisfy both the RF performance and low cost manufacture requirements. The objective of this research is to investigate flip chip technology for packaging of high-speed modulator on $LiNbO_3$ [8].

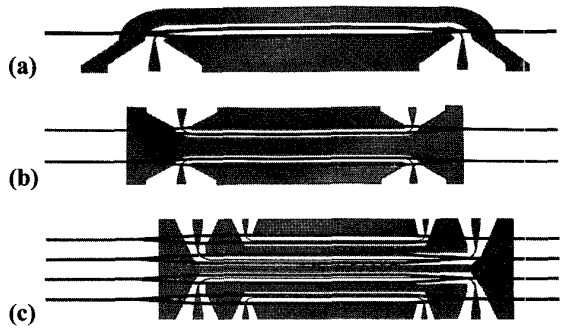

Figure 1. Diagrams of various MZI configurations: (a) single-electrode MZI, (b) Dual electrode MZI and (c) modulator array (4 MZI's).

This paper is structured as follows. In Section II, a background of flip chip technology is presented. Methods by which flip chip techniques could improve modulator packaging are also proposed. Section III presents an investigation of flip chip bonding on ceramic substrates. This preliminary investigation includes the flip chip bonding method and also RF characterization of the realized bonds. A benchmark of performance is thus established. Section IV presents a demonstration flip chip bonding of a ceramic substrate to a $LiNbO_3$ modulator electrode. Section V summarises this investigation and presents an assessment of the benefits this technology offers to modulator packaging.

II. Flip Chip Technology and Application to MZI Arrays

Flip chip technology has become popular in the manufacture of digital electronic devices and systems. The advantage of flip chip technology over other interconnects such as solder and wire bonds is that they are very compact. This increases device density and hence improves yield, but also increases speed, lowers power consumption and improves reliability [9 - 11]. It is proposed that similar benefits could be expected from the application of flip chip technology to high-speed opto-electronic communication devices [4, 7].

The flip chip bonding approach is conceptually fairly simple. Traditionally, to electrically connect microwave waveguides on two substrates, the two samples are aligned side-by-side and wire bonds are used to connect the two substrates. Flip chip bonding adds an extra dimension to this bonding process by enabling the chips to be bonded face to face. One sample is prepared with metallic 'bumps' that will

form the bonds. This sample is then 'flipped' over such that it is facing downward and is aligned to a second sample. The two samples are then brought into contact and a combination of pressure, heat and ultra-sonic vibration is used to fuse the bumps on the first substrate to the second substrate. There is great flexibility in the dimension and distribution of the bumps that define the bonds and this allows the flip chip technology to be applied to a broad range of bonding situations as well as being scalable to smaller and denser connections.

To illustrate the advantages that may be offered by flip chip bonding, a proposed improvement to the MZI array depicted in Figure 1(c) is presented in Figure 2. The RF electrodes are straightened as electrical connection can be achieved from above the device rather than from the chip edge. This offers several advantages. Firstly, the overall width of the device can be reduced to the width of the flip chip pad. This will greatly reduce the area required for each device. Further, the bonding process can be completed in a single step for all of the modulators in the array. This will significantly reduce the cost of manufacture.

Perhaps the most important advantage of this proposed flip chip approach is that the electrode on the $LiNbO_3$ surface is only that which is required for efficient modulation. All other signal transport and waveguide tapering required for interfacing external electronics can be implemented on a low loss microwave substrate flip chip bonded to the modulator devices. One such substrate is "CoorsTek ADS-96R" ceramic [12]. Ultimately, it may also be possible to Flip chip interface the modulator directly to a silicon electronic substrate, creating an extremely compact electro-optic subsystem.

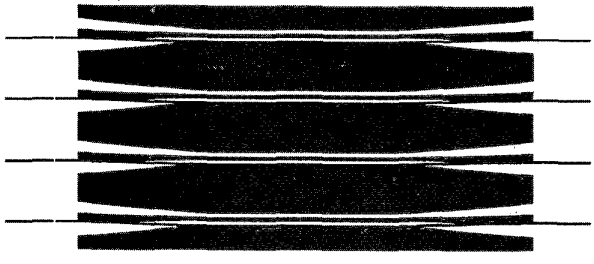

Figure 2. Proposed flip chip modulator array

III. Flip Chip Bonding: Ceramic-Ceramic 500μm Overlap

To begin the investigation it was decided to first examine the performance of the flip chip technique when bonding identical ceramic substrates. Ceramic substrates were chosen since they offer very low loss RF propagation and are also well behaved thermally. Bonding identical substrates also eliminated the issue of thermal mismatch.

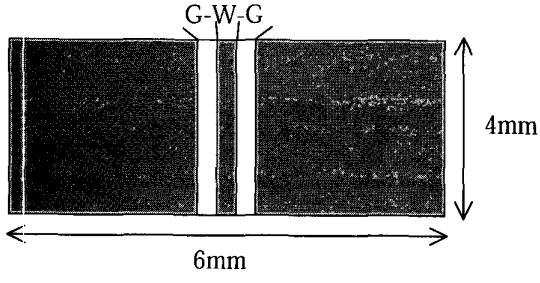

Figure 3: Schematic of coplanar ceramic substrate

A. Substrate Description

The substrates used were 4 x 6mm rectangles of ceramic ($\varepsilon_r = 9.6$) with a thickness of thickness of 635μm. These were patterned with 8μm thick gold coplanar waveguide (CPW) electrodes. Several coplanar configurations were investigated, but all were designed to be single mode and have impedance of 50Ω for frequencies up to 40GHz.

B. Bump Formation

Initially, the electroplated substrates were plasma cleaned in order to remove any organic contamination on the surface of the electrodes. The flip chip 'bumps' were then applied to the sample using the "Kulicke & Soffa (K & S) model 455" ball bonder and AW-6 gold wire with diameter of 24μm. Application was conducted at a temperature of 120°C. The excess gold wire was torn from the substrate to leave only the ball on the surface. A scanning electron micrograph (SEM) of a typical ball bump is presented in Figure 4(a).

The ball bumps were tested for the pull strengths in order to ensure good adhesion. The bond pull test was performed using the "Dage micro tester 22". Bond strengths in the range 4.5 – 5.3g were measured. These are well above those required for military certification (MIL-STD-883 [13]).

To ensure a flat surface with good contact during flip chip bonding, the gold 'bumps' were flattened into 'coins' as shown in Figure 4(b). This is using the "K& S model 455" ball bonder fitted with a coining tool. The height of the coined ball bumps was reduced to around 70μm. The ball bumps have a diameter of ~70-80μm after bumping and coining.

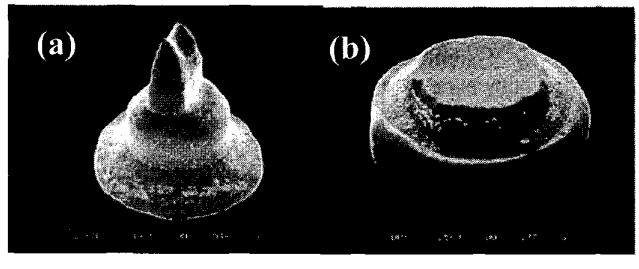

Figure 4. SEM picture of a gold ball bumps: (a) with the tail and (b) the tail gets coined before the flip chip bonding.

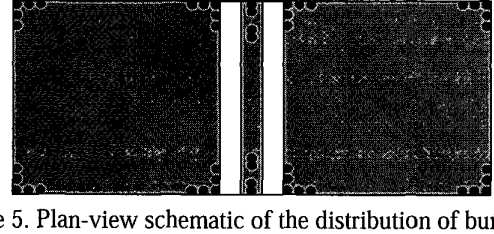

Figure 5. Plan-view schematic of the distribution of bumps for the first ceramic investigation (dots represent the ball bonds).

C. Flip Chip Bonding Procedure

For the first investigation a ceramic substrate with G-W-G of 170-400-170μm was selected. Bumps were distributed as shown in Figure 5. This arrangement was aimed to ensure good electrical contact and mechanical adhesion, especially in

the region close to the central coplanar electrode and also the corners of the device.

The device was flip chip bonded as shown in Figure 6 where the superstrates are individually placed on the input and output ports of the CPW device. These superstrates had the same geometry as shown in Figure 3. The superstrates were arranged with an overlap ~500μm to ensure mechanical stability.

The bonding was conducted on "A4 Fineplacer®-145" with a base heating plate and ultrasonic pick-up tool. A vacuum chuck held the bumped device to the pick-up tool. The individual superstrates were then lowered onto the ceramic device and bonded by applying a force of 160g/bump and an ultrasonic power of 250mW/bump at 200°C for 1.5 seconds. The temperature was increased from 40°C to 200°C at the rate of 3.2°C/sec. and gradually cooled to room temperature at the rate of 1°C/sec.

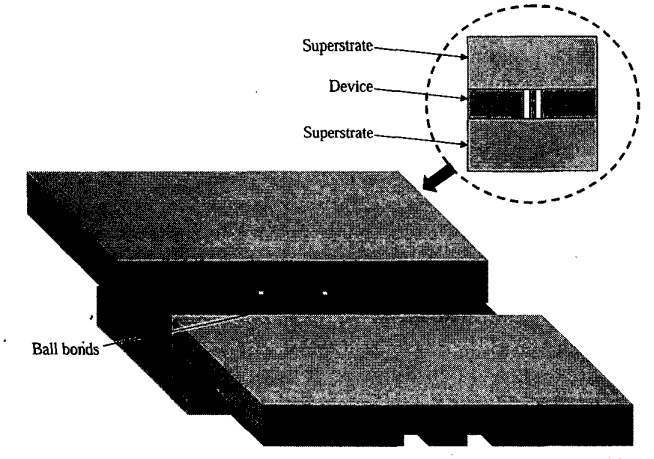

Figure 6. Configuration of a Ceramic-Ceramic-Ceramic flip chip (inset shows the top view of the device) with a G-W-G of 170-400-170μm.

D. Analysis of the Flip Chip Bond

The mechanical stability of the flip chip bond was tested for shear strength using the Dage bond pull tester on one end of the device. Shear strength was measured at 85g/bump and is above the required MIL-STD-883 specifications [13].

An SEM of a flip chip bond on the central electrode is presented in Figure 7. The plated coplanar structure with attached bonds can be seen in Figure 7(a). An enlarged portion of this image is presented in Figure 7(b). It can be seen that ball bump after flip chip bonding has a diameter of ~100μm and a height of ~30μm.

E. Electrical Characterisation

The aim of this investigation is to provide rugged low-loss electrical interface. It is thus necessary to characterize the RF performance of the realized bonds. The important characteristics are the RF insertion loss ($|S_{21}|$) and return loss ($|S_{11}|$) as a function of frequency.

The RF measurement set-up used in the investigation is shown in Figure 8. The RF performance of the devices were measured using a Wiltron Network Analyser 360B. The superstrates were probed using high frequency GGB Pico-probes (40A-GSG-400-Q). The measurement was conducted on a sheet of Flexflow RF absorber to minimize resonances due to the external environment. The probes were calibrated for operation in the frequency range of 1-38GHz. Measurements were performed at room temperature.

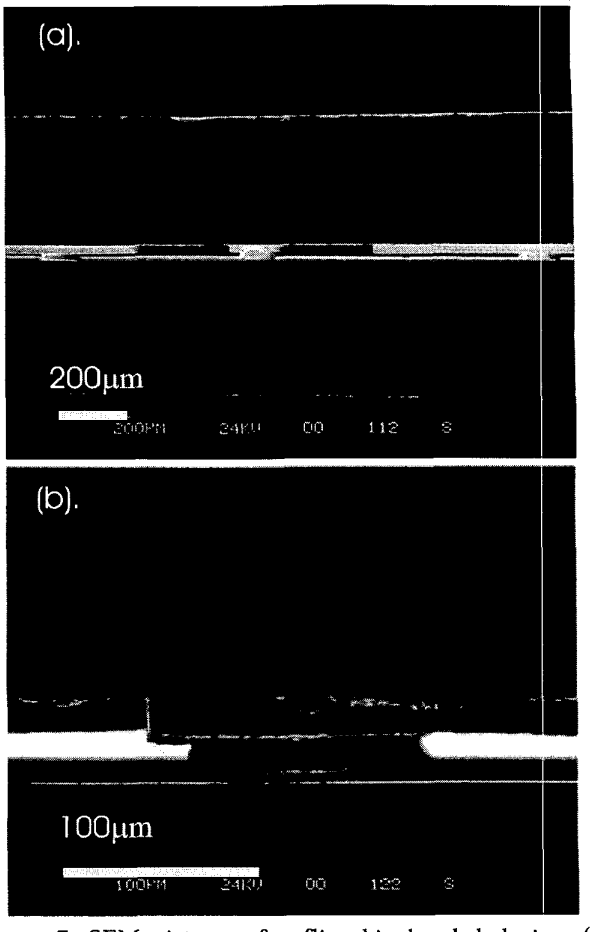

Figure 7. SEM pictures of a flip chip bonded device: (a) coplanar electrode and (b) enlarged image of bond on central electrode.

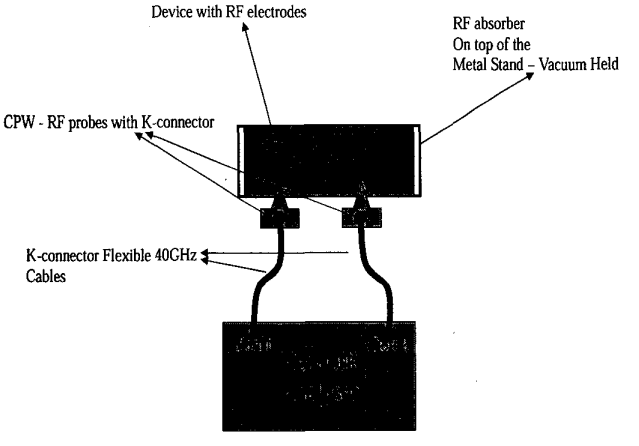

Figure 8. RF probe measurement set-up

To provide a reference, the RF properties of the coplanar substrate was analysed before flip chip bonding. These are presented in Figure 9. The insertion loss (S_{21}) is less than 1dB at 38GHz demonstrating that these substrates are relatively good quality for RF transmission and good return loss (i.e. approximately impedance of 50Ω) over the entire measurement frequency.

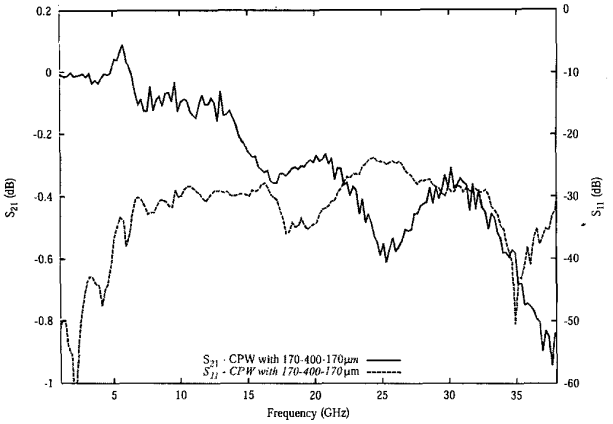

Figure 9. RF insertion loss ($|S_{21}|$) and return loss ($|S_{11}|$) of a single ceramic superstrate before flip chip bonding (G-W-G = 170-400-170μm).

The measured insertion loss and return loss of the flip chip sample is shown in Figures 10 and 11 respectively. In Figure 10, significant resonances were observed above 10GHz. Interestingly, the insertion loss of Figure 10 is only 1.2dB at 30GHz. This is approximately three times the insertion loss measured for a single substrate (as shown in Figure 9) suggesting that the insertion loss contributed by the flip chip bond itself is low even at 30GHz. It is proposed, therefore that the resonances are largely reactive and may thus be caused by reactive loading caused by mutual coupling of the overlapped substrates. A further experiment was undertaken to investigate this.

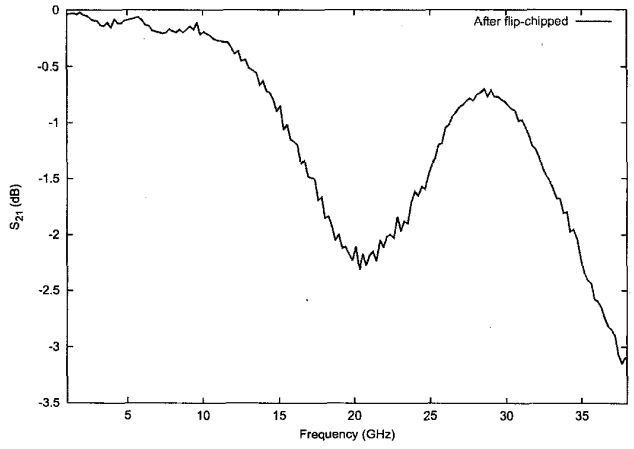

Figure 10. RF insertion loss ($|S_{21}|$) for the ceramic superstrate flip chip bonded onto a ceramic CPW as shown in Figure 6.

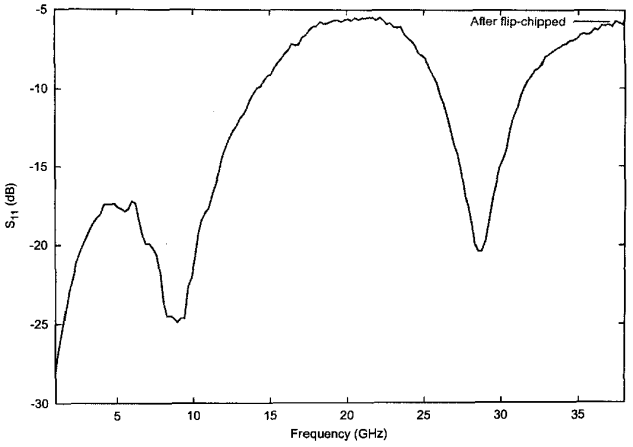

Figure 11. RF return loss ($|S_{11}|$) of the ceramic superstrate flip chip bonded onto a ceramic CPW device as shown in Figure 6.

III. Flip Chip Bonding: Ceramic-Ceramic 100μm Overlap

It was hypothesized that resonances observed in the RF responses of Figure 10 and 11 were the result of reactive loading caused by mutual coupling due to the 500μm overlap between the flip chipped electrodes (as shown in Figure 6). A new flip chip configuration is proposed where the overlap is minimized.

For this investigation, a coplanar electrode with G-W-G of 110-250-110μm was selected. Having established that the large number of bumps used in Figure 5 was in excess of that required to ensure a rugged device, approximately half the number of bumps were used in the present investigation. Bumps were placed on the perimeter of the electrode such that only a 100μm overlap would be required for bonding. The distribution of bumps is presented in Figure 12.

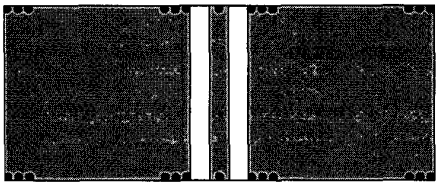

Figure 12. Bump distribution for 100μm overlap.

The bumping, coining, flip chip and RF characterization procedures were the same as those presented in Section II. The RF insertion loss and return loss for the flip chip bonded ceramic substrates with 100μm overlap are presented in Figures 13 and 14 respectively. It is evident that the resonances observed in Figures 10 and 11 have been eliminated leaving a relatively flat, low loss response. The predicted insertion loss calculated using the S-parameters of individual CPW devices on ceramic substrate prior to flip chip bonding are also presented in Figures 13 and 14. Thus, it can be observed that flip chip bonds have contributed minimal RF losses to the overall response.

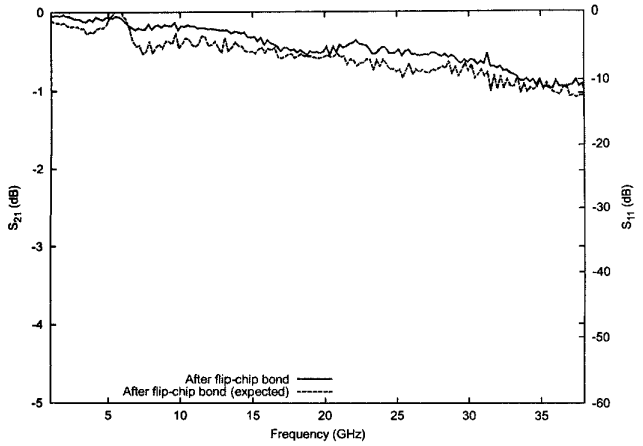

Figure 13. RF insertion loss ($|S_{21}|$) of the ceramic superstrate flip chip bonded onto a ceramic CPW device with 100μm overlap.

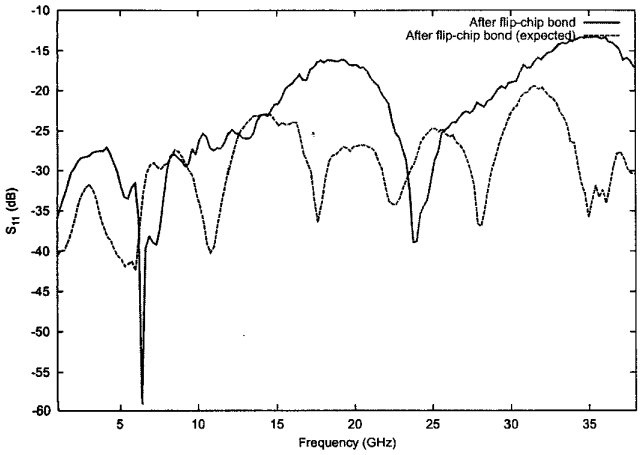

Figure 14. RF return loss ($|S_{11}|$) of the ceramic superstrate flip chip bonded onto a ceramic CPW device with 100μm overlap.

It can be concluded therefore that flip chip bonding can provide excellent bonding up to 38GHz. It is important, however, that the overlap between the substrates must be minimized to reduce mutual coupling and reactive loading. In future investigations care must be taken to accommodate for any reactive coupling between the substrates.

IV. Flip Chip Bonding: LiNbO3-Ceramic

Having established that flip chip bonding can provide excellent bonds between ceramic substrates up to 38GHz, it is now possible to begin investigation of flip chip bonding of a $LiNbO_3$ electrode to a ceramic substrate.

The modulator chip had length, width and thickness of 5.4cm, 2.0mm and 500μm respectively [4]. The electrode structure of the optical modulator used in this investigation is shown in Figure 15(a). It had an RF electrode length of 2.5cm and tapered to a G-W-G of 320-100-320μm at the edges.

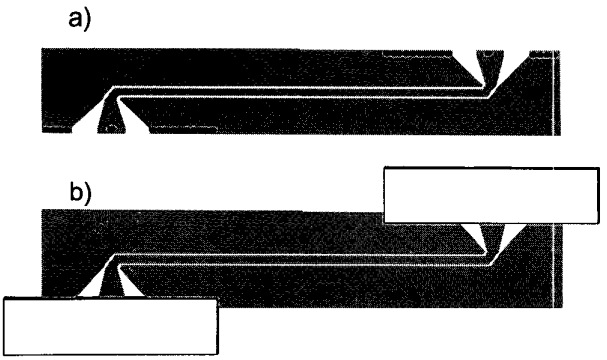

Figure 15. Plan view of the $LiNbO_3$ modulator electrode: (a) distribution of bumps and (b) flip chip bonded modulator with ceramic superstrates with G-W-G 170-400-170μm and 100μm overlap.

Bumps were distributed on the modulator electrode as shown in Figure 15(a). Bumps were placed only on the perimeter to minimize overlap between the modulator and superstrates was maintained at 100μm. This was done to minimize reactive loading as discussed in Section III.

The flip chip structure used is shown in Figure 15(b). Ceramic superstrates with G-W-G of 170-400-170μm were flip chip bonded to the $LiNbO_3$ using the technique and parameters described in Section II. It was anticipated that the shear strength of the bonds between the ceramic and $LiNbO_3$ substrates would be different than for the ceramic-ceramic bonds, however, since the shear strength test is destructive; it was not performed on this initial sample. A set of mechanical validation procedures will be conducted in a future investigation.

Figure 16 presents the RF insertion loss of the $LiNbO_3$ electrode probed on a sheet of microwave absorber, the response predicted by cascading two ceramic substrates with the measured modulator response and the actual measured flip chip response. The performance is evidently very similar to that predicted up to about 30GHz. Remarkably, above 30GHz, the measured flip chip performance is actually better than the un-bonded chip. Here substrate resonances begin to degrade the LiNbO3 electrode performance. The improved performance above 30GHz can thus be attributed to the lower surface of the $LiNbO_3$ being suspended in air during measurement rather than being in contact with microwave absorber. For a practical device, the substrate would be thinned from 500μm to 250μm to eliminate substrate resonance.

The RF return loss is shown in Figure 17. The responses for the measured bare chip, predicted flip chip and measured flip chip are again very similar up to around 30GHz. Again, above 30GHz the effect of microwave absorber on the substrate resonances is significant. Importantly, the return loss is below -10dB for all frequencies.

It can be concluded from this preliminary investigation that flip chip bonding can be used successfully to electrically interface $LiNbO_3$ chips up to 38GHz. An analysis of the mechanical properties of these chips is currently underway.

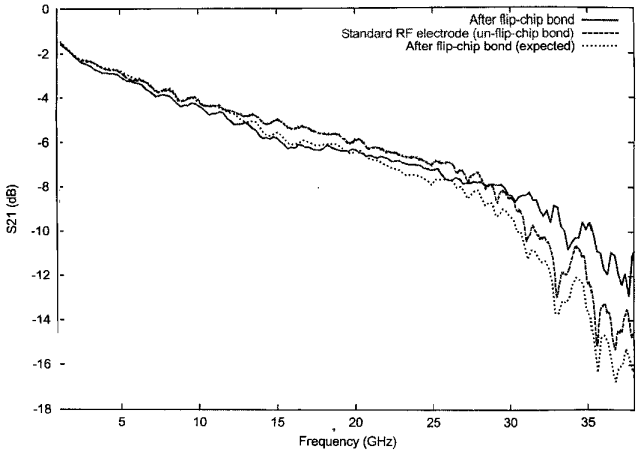

Figure 16. RF insertion loss ($|S_{21}|$) of the superstrate flip chip bonded onto an optical modulator

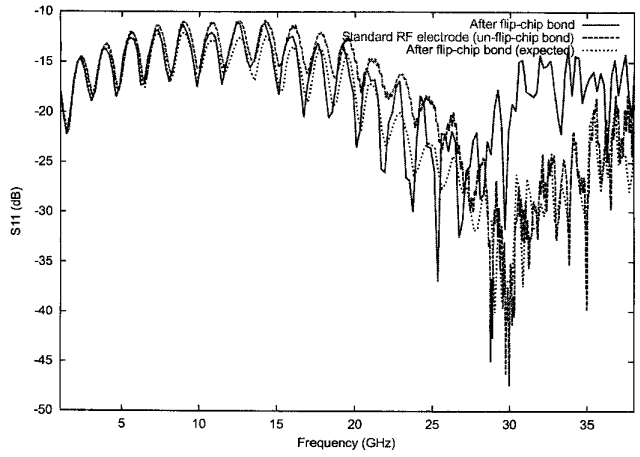

Figure 17. RF return loss ($|S_{11}|$) of the superstrate flip chip bonded onto an optical modulator

V. Conclusions and Future Work

The results presented in the paper demonstrate that the flip chip process introduces minimal degradation to the RF performance of the optical modulators. The investigation of flip chip interconnects were validated by bonding CPW superstrates onto ceramic substrates and also to $LiNbO_3$ devices respectively. It was found that care must be taken to minimize reactive loading due to mutual coupling. An overlap between the substrates of 100μm was found to provide good performance.

Establishment of the mechanical and thermal stability of the flip chip bonds will be essential if this technique is to be developed into a process suitable for device manufacture. Environmental characterization of flip chip bonded modulator devices is currently underway. Studies to optimize the bump dimensions, distribution and bonding parameters to enhance environmental stability will also be conducted.

Once the environmental stability of this process has been established, numerous research avenues can be pursued. Designs that will enable the RF substrate to act both as an electrical interface and a thermally matched mechanical mount will be of great benefit. The substrate could also accommodate RF amplifiers or other active and reactive components. These ancillary components could be attached using conventional wire bonding, surface mount or flip chip techniques.

Further research into the design of flip chip superstrates that can be bonded to multi-port modulator electrodes (such as that presented in Figure 2) should be investigated. The possibility of such parallel vertical connections is a unique advantage offered by the flip chip technique. Care must be taken in this design to minimize mutual coupling since significant overlap between the modulator chip and flip chip superstrate will be inevitable.

The demonstration of compact, low-loss flip chip bonds has also made practical the possibility of directly interfacing reactive components with modulator electrodes to realize high-frequency resonantly enhanced modulators as suggested in [14,15]. The low loss of the bonds ensures a high-Q resonance can be achieved, while the 30μm proximity of the superstrate to the substrate will enable relatively short cavity lengths such that high-frequency operation can be attained.

VI. Acknowledgments

The authors would like to thank the Australian Photonic CRC for funding this investigation. We would also like to thank DSTO for providing their facilities in order to perform the flip chip investigation. Mr. Michael Parker provided assistance in the use of the RF measurement facility at DSTO. Dean Pavlickovski, Paul Jones, Yuxum Cao and Chiping Wu for fabricating the superstrates, optical modulators and the characterisation of the devices using the Microelectronic Materials and Technology Centre (MMTC) at RMIT University.

VII. References

[1]. N. Dagli, "Wide-Bandwidth Lasers and Modulators for RF Photonics", *IEEE Trans. Microwave Theory Tech.*, vol. 47, no. 7, pp. 1151 – 1171, July 1999.

[2]. E. L. Wooten and et al, "Review of Lithium Liobate Modulators for Fiber-optic Communcations Systems", *IEEE J. Selected Topics in Quantum Electron.*, vol. 6, pp. 69 - 82, Jan/Feb 2000.

[3]. T. Nakazawa, "Low Drive Voltage and Broad-Band $LiNbO_3$ Modulator", *International Topical Meeting on Microwave Photonics (MWP' 99)*, Technical Digest, pp. 17 – 20, 1999.

[4]. M. W. Austin, "Packaging of 40GHz Optical Modulators with MMIC Pre-Amplifiers", *Proc. 54th Electronics Components and Technology Conference*, pp. 289 – 291, San Diego, California, 2002.

[5]. "Properties of Lithium Niobate", *EMIS Datareviews Series No.5*, INSPEC publication.

[6]. K. Goverdhanam, "Effect of Substrate Modes in 40Gbit Travelling Wave LiNbO3 Modulators", *IEEE MTT-S Digest*, pp. 1285 – 1288, 2002.

[7]. R. A. Becker and B. E. Kincaid, "High Performance, High-Isolation Optical Guided-Wave Device Arrays", *IEEE J. Lightwave Technol.*, Vol. 17, No.2, pp. 260 – 266, Feb. 1999.

[8]. K. Yoshida and et al, "Design and Performance of Superconducting Circuits for $LiNbO_3$ Optical Modulator and Switch", *IEEE Trans. Applied Superconductivity*, Vol. 13, no. 2, pp. 1027 – 1030, June 2003.
[9]. D. Styblo and et al, "Gold-On-Gold Flip Chip", Suss MicroTec, pp. 49 – 53, http://www.suss.com/devicebonder/newsletter/past/6/article3.htm, 2003.
[10]. M. Wale and M. Goodwin, "Flip Chip Bonding Optomizes Opto-ICs", *IEEE Circuits and Devices Magazine*, pp. 25 – 31, Nov. 1992.
[11]. A. Jentzsch and W. Heinrich, "Theory and Measurements of Flip Chip Interconnects for Frequencies up to 100 GHz", *IEEE Trans. Microwave Theory Tech.*, vol. 49, pp. 871 – 877, May 2001.
[12]. Ceramic substrate - ADS-96R, http://www.coorstek.com
[13]. MIL-STD-883, http://www.dscc.dla.mil/Offices/Doc_Control
[14]. T. G. Nguyen, A. Mitchell, and Y. S. Visagathilagar, "Investigation of Resonantly Enhanced Modulators on $LiNbO_3$ using FEM and Numerical Optimization Technique", *IEEE Journal of Lightwave Technology*, paper accepted for publication, Jan. 2004.
[15]. Y. S. Visagathilagar, A.Mitchell, and R. B. Waterhouse, "Fabry-Perot Type Resonantly Enhanced Mach-Zehnder Modulator", *International Topical Meeting on Microwave Photonics (MWP' 99)*, Technical digest, pp. 17 - 20, November 1999.